PNAS RESEARCH ARTICLE | BIOPHYSICS AND COMPUTATIONAL BIOLOGY

3D nanoscale imaging of amyloid-β oligomer interactions with extracellular vesicles by cryo-ET

Anum Khursheed[a], Qi Shang[a], Hui Zhang[a], Yao Tian[a,b], Piotr Szwedziak[c], Vladimir A. Volkov[a], and John H. Viles[a,1]

Affiliations are included on p. 6.

Edited by G. Marius Clore, National Institutes of Health, Bethesda, MD; received March 24, 2026; accepted June 8, 2026

Central to Alzheimer's disease pathology are prefibrillar oligomer assemblies of amyloid-β (Aβ) peptide. A widely discussed hypothesis proposes that amyloid-β oligomers insert into neuronal lipid membranes, disrupting their integrity and causing a loss of cellular homeostasis in Alzheimer's disease. This membrane disruption is believed to be a major source of Aβ-induced neurotoxicity. Cryo electron tomography (cryo-ET) has facilitated 3D nanoscale imaging of Aβ-membrane interactions under near-native conditions. Analyses of small extracellular vesicles (sEVs) reveals that Aβ oligomers including annular and curvilinear extended oligomers (CLEOs) exhibit extensive binding to cell-derived lipid membranes, including insertion into and carpeting of the lipid bilayer. Notably, these oligomeric assemblies were also internalized and concentrated within the cell-derived exosomes and other small sEVs. Enrichment of Aβ oligomers within the vesicles typically ranged between 5 to 20 times the external Aβ levels depending on the vesicle size and curvature. In contrast, monomeric and fibrillar forms of Aβ displayed minimal membrane interaction. Once internalized CLEOs appear to be trapped in an oligomeric form and do not readily go on to form fibrils. Studies with vesicles of brain lipid extract indicate the Aβ internalization does not require the presence of a membrane protein. Our in vitro studies underscore the membrane-disruptive capacity of oligomeric Aβ species and suggest a role of sEVs in concentrating toxic Aβ oligomers and transporting oligomers across the brain interstitium.

Alzheimer's | annular | protofibril | membrane | cryo-EM

Significance

Alzheimer's disease accounts for over two-thirds of dementia cases worldwide. A key factor in Alzheimer's disease pathology is the hydrophobic peptide, amyloid-β (Aβ), which self-assembles into neurotoxic oligomers found in patients' brains. It is yet to be established the mechanism by which Aβ causes neurotoxicity. Using cryo electron tomography, we examined how Aβ interacts with cellular lipid membranes under near-native conditions. We obtained nanoscale, three-dimensional images showing small Aβ oligomers embedded within membranes. Aβ oligomers are also concentrated inside vesicles which suggests a mechanism by which Aβ can spread across the brain. These in vitro studies reveal extensive incorporation of Aβ oligomers into lipid bilayers, illustrating how membrane integrity and cellular homeostasis may be disrupted, and so contribute to neuronal loss.

Alzheimer's disease (AD) is the most common form of dementia (1). There is a large body of evidence that links the overproduction, increased aggregation, or reduced clearance of the amyloid-β (Aβ) peptide with AD pathology (2, 3). However, the precise mechanism by which Aβ exerts neurotoxicity is still hotly debated, although it is established prefibrillar assemblies, loosely described as Aβ oligomers, 9-200 kDa in weight, are responsible for neurotoxicity (4–8). One hypothesis involves the direct interaction of Aβ oligomers with cellular membranes (9–12). Aβ prefibrillar assemblies have been shown to compromise membrane integrity, leading to disrupted Ca^{2+} homeostasis and eventual cell death (13–16). In particular, Aβ oligomers cause Ca^{2+} influx in cellular models (12, 17–19) and dye release in synthetic vesicles (20, 21). It is believed the membrane permeability is caused by the insertion of oligomers and curvilinear extended oligomers (CLEOs) in the lipid bilayer (9–11, 22–24). In addition, ring-shaped annular Aβ oligomers are believed to form ion-channel pores across the membrane that also disrupt cell homeostasis (25–27). Alternatively, Aβ may disrupt cellular function by binding to membrane receptors (28–31).

Although much of Aβ is observed extracellularly, intracellular accumulation of Aβ is linked with synaptic and neuronal dysfunction in AD pathology (32–34). Aβ aggregation is linked to cellular uptake and Aβ cytotoxicity (35). The mechanism of Aβ uptake (36) might be via glutamate receptors (37) or acetylcholine receptors (38) or via an endocytic pathway (39–41). Protein independent diffusion of Aβ across the membrane has also been suggested (42).

Nano-scale imaging of Aβ interactions with the lipid bilayer have been restricted to synthetic lipids. In particular, there have been studies using atomic force microscopy (AFM) of supported lipid bilayers and our cryo electron tomography (cryo-ET) study of a simple synthetic lipid vesicles model (9–11, 22, 27, 43). Cryo-ET imaging of amyloid fibrils postmortem has been reported; however, oligomers were not identified (44). We wanted to extend these studies to cell-derived lipid bilayers. To achieve this, we have isolated small extracellular vesicles (sEVs) from the cellular medium. The relatively small size of the cell derived vesicles makes them amenable to nano-scale imaging using cryo electron tomography (cryo-ET), without the need of focused ion beam (FIB) milling, which is typically required for whole-cell studies (44). Vesicles are secreted by most cell

Author contributions: A.K. and J.H.V. designed research; A.K., Q.S., and Y.T. performed research; A.K., Q.S., H.Z., P.S., and V.A.V. analyzed data; and A.K. and J.H.V. wrote the paper.

The authors declare no competing interest.

This article is a PNAS Direct Submission.

[1]To whom correspondence may be addressed. Email: j.viles@qmul.ac.uk.

This article contains supporting information online at https://www.pnas.org/lookup/suppl/doi:10.1073/pnas.2610068123/-/DCSupplemental.

Published July 14, 2026.

types, including those in the central nervous system (45). Small EVs lipid composition largely reflects that of a typical lipid bilayer from the plasma membrane and so also contains membrane associated proteins (46–48). These properties make the sEVs, which include exosomes, a good model to study Aβ interactions with cell membranes.

In vivo, sEVs, including exosomes, traffic both extracellular Aβ and also facilitate intercellular trafficking of Aβ in Alzheimer's disease (AD) (49–54) and are associated with AD pathology (55, 56). Additionally, in vitro sEVs, including exosomes, have been shown to accelerate the rate of Aβ assembly (57).

Here we aim to visualize, at the nanoscale, the interaction of Aβ42 in various assembly forms with cell derived sEV's. We show that only Aβ as oligomers insert into the lipid-bilayer. In contrast to previous studies with synthetic vesicle models, there is a profound internalization and concentrating of Aβ oligomers and annular assemblies within the vesicles. It is now clear Aβ, in oligomeric forms, are able to cross the cell membrane and thus be incorporated and transported by sEVs.

Results and Discussion

Characterizing Cell Derived Vesicles and Aβ Assemblies. To investigate Aβ42 membrane interactions, sEVs were isolated from HEK-293 cells using a centrifugation protocol (58). HEK cells were chosen because they mimic neuronal properties and we have previously used HEK cells to monitor Aβ ion-channel pore formation using patch-clamp electrophysiology (12, 26). The isolated sEV, which include exosomes, were characterized by cryo-EM and cryo-ET imaging. The isolation process generates intact spherical vesicles that are typically unilamellar and occasionally multilamellar. The vesicles appear empty with very few detectable structures within, *SI Appendix*, Fig. S1. The vesicles (sEV) have a median diameter of 120 nm and typically range from 30 to 300 nm. The lipid bilayer thickness is 5.4 ± 0.1 nm.

We wanted to study the impact of three different assembly forms of Aβ42 on the lipid bilayer: i) chromatographically pure monomeric Aβ42; ii) a mixture of prefibrillar structures at the end of the lag-phase of assembly described as oligomers; and iii) fibrillar Aβ42 formed at the equilibrium stage of assembly. We have recently reported an extensive characterization of lag-phase assemblies, using a range of imaging techniques (12). Aβ42 taken from the end of the lag-phase contains a heterogeneous mixture of small oligomers, together with CLEOs and a smaller number (typically *ca*. 5 to 10%) of annular, ring-shaped, oligomers. Cryo-ET images of these different assembly forms and their dimensions are summarized in Fig. 1 and are in close agreement with temporal AFM and cryo-EM imaging we have previously reported. Importantly a consistent 2.8 nm cross-section diameter of the Aβ42 CLEOs is observed (12). No attempt was made to isolate this dynamic lag-phase oligomeric mixture, which also contains appreciable monomeric Aβ. This reflects the in vivo situation in which Aβ is a heterogenous mixture.

Imaging Aβ-Membrane Interactions. The different assembly forms of Aβ42 have very different impacts on the lipid membrane of the cell-derived sEVs, Fig. 2. Aβ42 oligomeric assemblies, including CLEOs, were observed to extensively associate and "carpet" the membrane of the sEVs, Fig. 2*C* and *SI Appendix*, Fig. S2*C*. In contrast, incubation of fibrillar Aβ42 with sEVs exhibit minimal membrane interaction, Fig. 2*D* and *SI Appendix*, Fig. S2*D*. Aβ42 monomers (4.5 kDa) are too small to be imaged by cryo-EM as individual peptides, however the membrane images of vesicles incubated with Aβ42 monomers are indistinguishable from

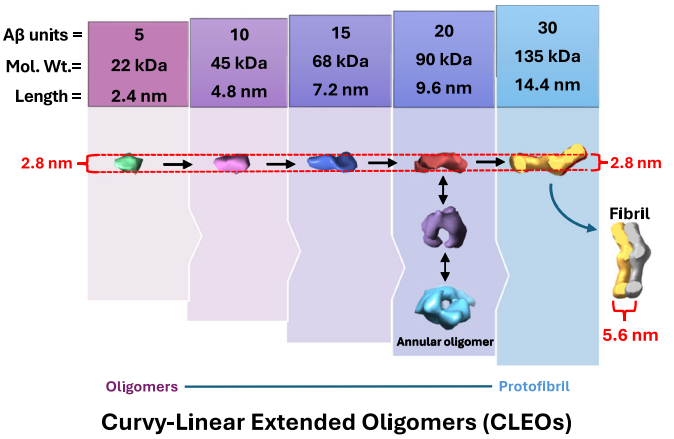

Fig. 1. Prefibrillar assemblies of Aβ42, imaged by cryo-ET. CLEOs and the annular oligomers dominate in the lag-phase before fibril formation. The number of Aβ molecules is suggested by the dimensions. These structures are three-dimensional reconstructions obtained by cryoelectron tomography.

vesicles in buffer alone, Fig. 2 *A* and *B* and *SI Appendix*, Fig. S2. This suggests there is little accumulation of Aβ42 monomer at the membrane or disruption of the bilayer by Aβ42 monomers. As such, the Aβ42 monomers effectively act as a nonamyloid control for these studies.

Cryo-EM images hint that Aβ42 oligomers cross the bilayer and are internalized by the vesicle. However, cryo-EM cannot distinguish between Aβ oligomers on the surface of the vesicle or within the sEVs, Fig. 2*C*. For this reason, we chose to use cryo-ET, which can visualize the whole vesicle in three dimensions. In this approach the 3-D tomograms, and each 2-D slice, produce excellent contrast, of the vitrified sample, without heavy-metal staining, and can distinguish the membrane surface and any internal assemblies within the vesicle, if they are present. There were three independent sEV preparations in which vesicles were incubated with Aβ42 oligomers

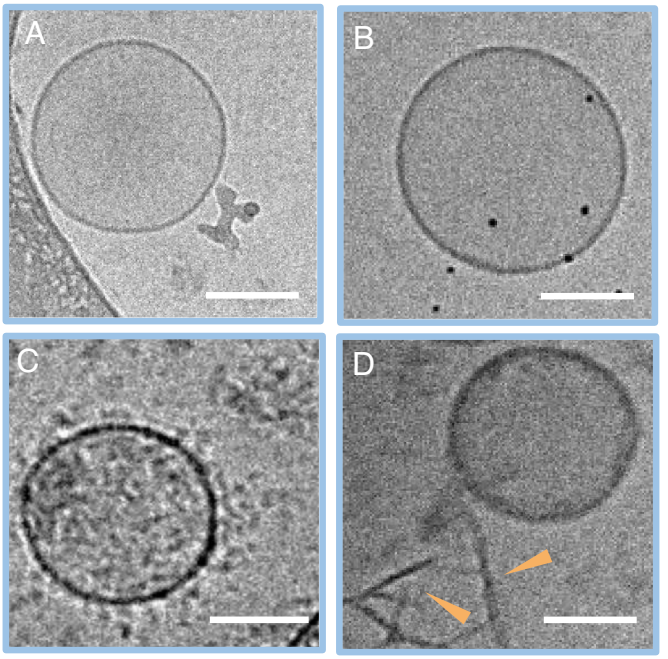

Fig. 2. Cryo-EM images of sEVs in the presence of $A\beta_{42}$ assemblies. PBS buffer (*A*); $A\beta_{42}$ monomers, black dots are gold particles (*B*); lag-phase $A\beta_{42}$ oligomers (*C*); and $A\beta_{42}$ fibrils (*D*). sEVs extracted from HEK-293 cells in PBS buffer at pH 7.4. (Magnification 50k×, Scale bar, 50 nm.) Orange triangles indicate fibrils.

and cryo-ET images collected, together with accompanying controls (sEV with no Aβ42). Consistently similar observations were made for all three datasets. Analysis of the reconstructed 3D tomograms reveals that sEVs, in the absence of Aβ42, exhibit a smooth membrane, with a spherical appearance and an interior indistinguishable from the ice background, Fig. 3*A* and *SI Appendix*, Fig. S1. Cell derived sEVs exposed to prefibrillar Aβ42 oligomers displayed extensive binding to the membrane surface and insertion into the bilayer, Fig. 3*B* and *SI Appendix*, Fig. S3. Furthermore, the cryo-ET images do indeed indicate extensive internalization of the assemblies inside the vesicle. The appearance and dimensions of these internalized assemblies match those of Aβ42 oligomers and possess a consistent diameter for most of the structures of 2.8 ± 0.1 nm, *SI Appendix*, Fig. S4, which is characteristic for Aβ42 CLEO's (12). These internalized CLEOs are also shown as 3D surface-rendered structures, *SI Appendix*, Fig. S4. 3D tomograms are shown as Movies S1 and S2, sEVs are shown with, and without, the presence of Aβ42 oligomers. The movies show Aβ oligomers inserting into the membrane bilayer and are also internalized within the vesicles.

The Aβ42 CLEOs embedded on the surface of the sEVs and internalized are particularly well visualized in the rendered 3D tomograms, Figs. 3 and 4 and *SI Appendix*, Fig. S4. There is a difference in the grayscale density of the oligomers relative to the density of the lipid bilayer. This difference in density enables the visualization of Aβ42 oligomers embedding and traversing the lipid bilayer. This is highlighted in Fig. 5 *A–C*, where 3D rendered images are shown with two density thresholds. Aβ CLEOs are well resolved emerging from the surface of the membrane, often orthogonal to the membrane surface. The CLEOs can protrude from both the outer- and inner-surface of the membrane, Fig. 5 *A* and *B*. While other CLEOs appear embedded parallel to the membrane surface, Fig. 5*C*. The presence of Aβ42 oligomers embedded within the lipid bilayer is visualized as a z-stack of tomogram slices, 6.7 nm apart. As we image consecutive slices of the lipid membrane in the z-stack, we observe different CLEOs within the membrane appearing, as shown in *SI Appendix*, Fig. S5*A*. Further examples of CLEOs emerging out of the inner and outer leaflet of the bilayer are shown in *SI Appendix*, Fig. S5 *C* and *D*. These images show that the Aβ oligomers can embed and traverse the bilayer.

The extensive interaction of Aβ42 oligomers with the lipid-bilayers disrupts the phospholipid packing, leading to ion permeability such as Ca^{2+}. We have used a Ca^{2+} sensitive fluorescent dye, Fluro4, which becomes de-esterified and sensitive to Ca^{2+} within the HEK293 cells. Addition of Aβ42 oligomers (5 μM) into the extracellular medium causes a large influx of Ca^{2+} into the cell cytosol, within a few seconds, while Aβ42 monomers or fibrils have minimal impact on Ca^{2+} influx, Fig. 5 *C* and *D*. Further examples of Ca^{2+} influx in which only Aβ42 oligomers are added to the extracellular medium are shown in *SI Appendix*, Fig. S6. In a dose–response curve, doubling the amount of Aβ42 oligomers added to the cell medium, causes the Ca^{2+} induced fluorescence to double in intensity, *SI Appendix*, Fig. S6.

To quantify the extent of Aβ42 oligomer binding and incorporation into sEV membranes and lumens, gray-value profiles were generated across 2-D slices from tomograms. Aβ free sEVs exhibit a uniform lipid bilayer with similar densities for the inner and outer-leaflet, *SI Appendix*, Fig. S7*A*. In contrast, sEVs incubated with Aβ42 oligomers displayed increased gray-value intensities

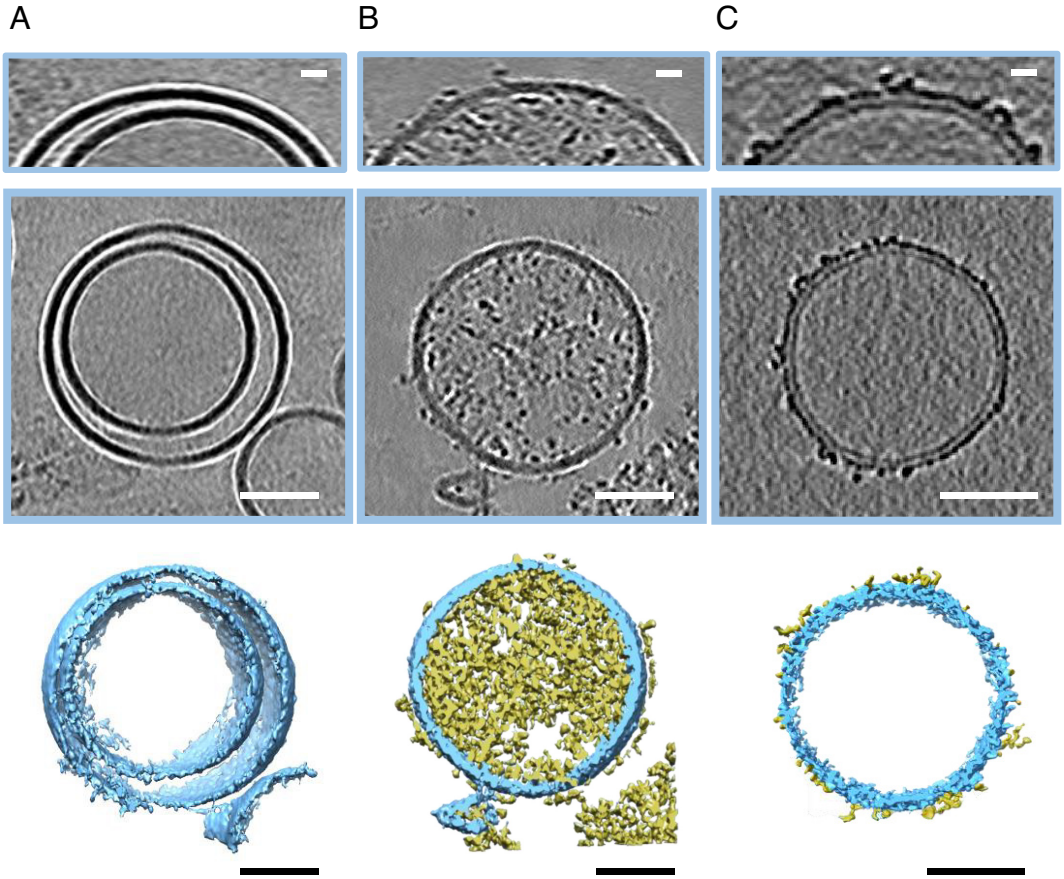

Fig. 3. $A\beta_{42}$ prefibrillar assemblies with sEVs and synthetic lipid vesicle. Cryo-ET 2D slices of sEVs along with their 3D rendered model in the absence (*A*), presence of $A\beta_{42}$ oligomers (20 μM) (*B*) and synthetic lipid vesicles with $A\beta_{42}$ oligomers (*C*). (Scale bar, 50 nm, magnification 53k×.)

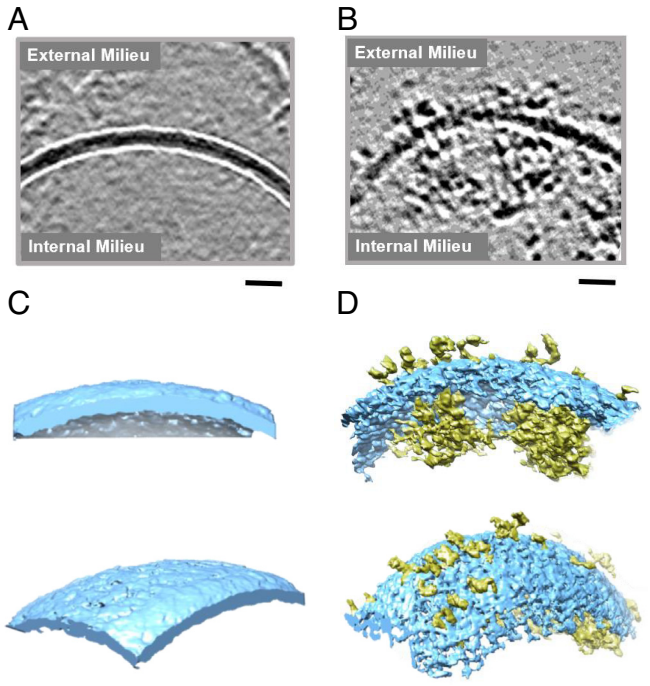

Fig. 4. $A\beta_{42}$ Oligomers interaction with sEVs, imaged by cryo-ET. Vesicle in absence of Aβ (*A*). In presence of $A\beta_{42}$ oligomers and CLEOs (*B*). Extensive carpeting and internalization of the $A\beta_{42}$ assemblies within the sEVs. Tomogram slice 6.7 nm thick (*A* and *B*). Associated rendered 3D tomogram (*C* and *D*). [Scale bar, 10 nm (black).]

and the inner membrane leaflet showed heightened density relative to the outer-leaflet. This insertion and surface carpeting by Aβ42 oligomers causes an apparent increase in membrane thickness, as observed in the gray-value profiles, *SI Appendix*, Fig. S7*B*. The membrane thickness for Aβ-free vesicles is 5.4 ± 0.1 nm, while the lipid bilayer in the presence of monomeric Aβ42 has a similar thickness of 5.2 ± 0.2 nm. There is an apparent increase in membrane thickness to 7.0 ± 0.4 nm in the presence of Aβ42 oligomers caused by Aβ42 oligomers carpeting the membrane surface. The embedded oligomers cause a reduction in density of phospholipids bilayer.

The other prefibrillar assemblies also observed in lag-phase Aβ42 preparations are annular in appearance. These distinctive ring-shaped structures are typically 6.5 nm in external diameter (12, 27). The annular assemblies are less abundant than CLEOs but are believed to be responsible for ion-channel pores characterized by large membrane conductance, these typically take between 5 to 10 mins to become active, after exposure to the cell membrane (26). Imaging annular structures embedded in the membrane is a challenge as there is only a small difference in density of the annular Aβ and the membrane itself. However, we were able to image the occasional annular structure which appears to be embedded in the membrane in the upper tomogram slices of the vesicle, Fig. 6*A*. Cryo-ET images of annular structures were also observed both external and internalized by the sEVs, Fig. 6*B* and *SI Appendix*, Fig. S8. These annular structures may have trafficked across the membrane or have formed from CLEOs within the vesicle. Annular structures have also been reported to embed in supported lipid bilayers, as imaged by AFM (27).

Aβ Oligomers Internalization. We were surprised by the observation of extensive internalized Aβ oligomers, including CLEOs, within the sEV's. Our previous study using synthetic vesicles showed Aβ oligomers carpeting only the outer-leaflet and were not internalized (11). This very different behavior for synthetic membranes was confirmed for Aβ42 oligomer preparations, Fig. 3*C*. For these synthetic large unilamellar vesicles (LUVs), (composition: PC;

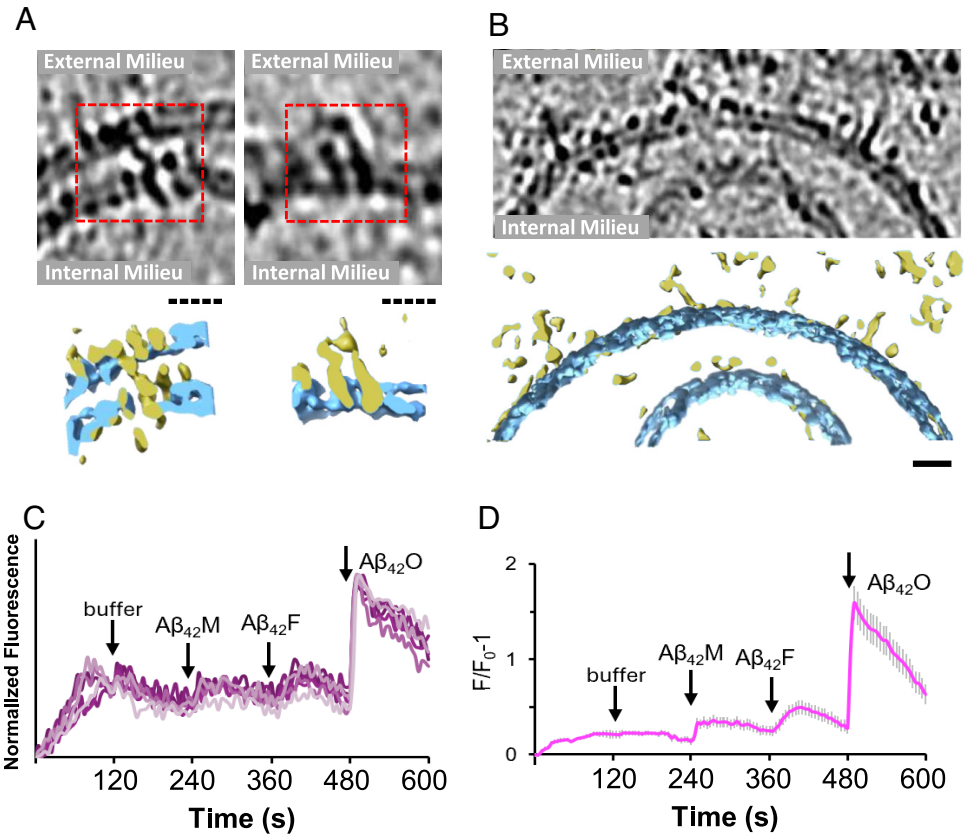

Fig. 5. $A\beta_{42}$ Oligomers insertion within lipid membranes and Cellular Ca^{2+} influx. Aβ42 oligomers inserting into sEVs membrane (*A*). Extensive insertion of $A\beta_{42}$ assemblies within the TBLE vesicle membrane, both orthogonal and parallel to membrane (*B*). The 3D rendered images are shown at two gray-scale intensities. The low highlights lipid bilayer (blue). The greater intensity highlights Aβ42 oligomers (yellow). [Scale bar, 10 nm (black).] Fluo-4 fluorescence traces detecting intracellular Ca^{2+} changes following sequential additions of buffer, Aβ42 monomers (Aβ42M), Aβ42 fibrils (Aβ42F), and Aβ42 oligomers (Aβ42O) (*C* and *D*). Representative fluorescence traces from six individual cells are shown (*C*). Mean Fluro-4 Ca^{2+} response from 127 cells, presented as mean ± SEM (*D*).

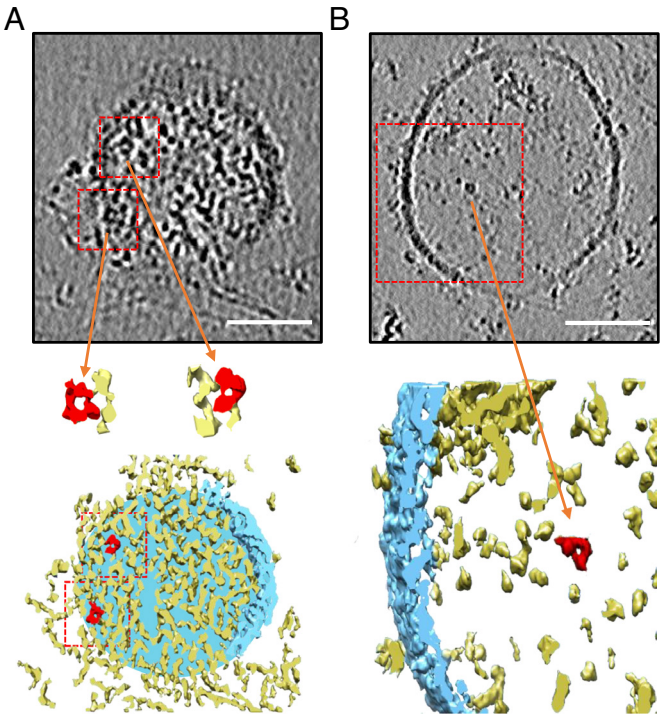

Fig. 6. Annular oligomers embedded and within extracellular vesicles. Cryo-ET tomogram slices showing Aβ42 annular assemblies localized on the surface of the sEV membrane, the top of the vesicle is shown (*A*), and internalized oligomers including annular oligomers (*B*). (Scale bar, 100 nm.) Three-dimensional rendering highlighting annular oligomers are in red, the other oligomers (CLEOs) with greater intensity are in yellow.

cholesterol; and GM1 - 68:30:2 by weight) Aβ oligomers are clearly observed carpeting the outer-leaflet of the lipid bilayer, but there is no evidence of internalization of the Aβ oligomers for these synthetic LUVs.

The distribution of Aβ oligomers (CLEOs) inside and outside the cell-derived vesicles suggests that not only are the Aβ oligomers internalized but the sEVs have the effect of concentrating Aβ assemblies inside the vesicle. To quantify this concentrating effect we have compared, gray-value intensities within and outside the sEVs, see *SI Appendix*, Fig. S9, and tabulated these for a number of vesicles, *SI Appendix*, Table S1. Tomogram slices of the same thickness through the middle of vesicles indicate densities above the background ice, and have a typical median coverage of 39%, *SI Appendix*, Table S1. While the presence of Aβ assemblies outside the vesicles have a less than 4% coverage. The interquartile range of coverage is between 20 to 40% within the vesicles, while using the same tomograms and thresholds the coverage of Aβ42 oligomers outside the vesicle is just 3 to 4%. Control vesicles, with no Aβ present, show no difference in gray-value density inside or outside the vesicle, *SI Appendix*, Table S1. This indicates, after a 2-h incubation time, CLEOs are concentrated within the vesicle by typically a median factor of ten. The vesicles have the effect of attracting, internalizing, and concentrating Aβ oligomers. It is also notable that smaller vesicles tend to have a greater density of internalized Aβ oligomers, *SI Appendix*, Table S1. Enrichment of Aβ oligomers within the vesicles ranged between fivefold for the larger vesicles (245 nm diameter) to 20-fold enrichment for the smaller vesicles (33 nm diameter). A plot of Aβ density internalized *versus* vesicle diameter indicates a doubling of oligomer density between vesicles of 120 nm and those of 60 nm diameter, *SI Appendix*, Fig. S10. The high concentration of Aβ oligomers within the sEVs is illustrated in a 3D rendered tomogram, shown as a Movie S3.

It is interesting to note that the concentrating effect of the vesicles on oligomers suggest that transport of Aβ oligomers into the vesicle is favored over movement out of the vesicle. This may be due to differences in lipid composition or phospholipid packing for the inner- and outer-leaflet of the cell derived vesicles. The differential internalization for smaller vesicles may be attributed to greater curvature within the membrane for the smaller (<60 nm in diameter) vesicles and/or a higher surface area to volume ratio for the smaller vesicles, which could facilitate more extensive binding and internalization of Aβ oligomers. This observation aligns with previous reports suggesting that the size of sEVs may influence their cargo loading efficiency and protein aggregation propensity (49, 55, 59) which suggests membrane curvature plays a crucial role in Aβ retention within sEV's (60). The internalization of Aβ oligomers is in agreement with a previous low-resolution fluorescence microscopy study that indicated Aβ oligomers are trafficked across the cell plasma membrane (35). Aβ oligomers have been shown to go on and interact with subcellular compartments such as mitochondria (32–34).

Next the question arises as to why only the cell derived vesicles internalize Aβ42 oligomers but synthetic vesicles containing PC; cholesterol and GM1, do not. The vesicle size and membrane curvature are very similar and images of EV's do not show any budding of the membrane. The internalization might therefore be due to different membrane phospholipid composition, which might facilitate membrane fluidity and the movement of oligomers, including CLEOs, across the bilayer. Alternatively, a protein binding partner may assist in Aβ internalization. To this end we generated synthetic vesicles from total brain lipid extracts (TBLE). This lipid mixture contains a more diverse range of phospholipids but lacks membrane associated proteins. Using cryo-ET we imaged TBLE vesicles incubated for 2 h with Aβ42 oligomers. Unlike the LUVs containing just PC; cholesterol; GM1, these synthetic TBLE vesicles do exhibit Aβ oligomers trafficking across the lipid bilayer with Aβ oligomers clearly present within the vesicles, *SI Appendix*, Fig. S11. These include annular oligomers visible inside the vesicles and within the bilayer, *SI Appendix*, Fig. S12. Importantly, these observations indicate that Aβ oligomers can traffic across the membrane but do not need a membrane-protein-binding partner to facilitate this behavior.

In contrast to Aβ monomers and fibrils, Aβ oligomers have a specific conformation that facilitates insertion and translocation across the membrane. The charge residues on Aβ will be attracted to the phospholipid head groups while penetration into the membrane is facilitated by exposed hydrophobic residues at the ends of the β-sheet rich CLEOs, believed to have a cross-β arrangement (12). The more rigid longer fibrils do not readily penetrate the membrane, only the less abundant exposed ends of fibrils have occasionally been imaged interacting with the lipid-bilayer. The heightened internalization of Aβ for smaller vesicles, with greater membrane curvature, suggest that the strained lipid-packing favors internalization of the oligomers rather than export of oligomers out of vesicles.

We wondered if once Aβ oligomers are internalized and concentrated, in the vesicles, would they then go on to form fibrils. To this end we incubated Aβ with vesicles for extended periods of time, expecting to observe the oligomers being replaced by fibrils. The addition of Aβ oligomers to the vesicles shows almost immediate substantial binding to the membrane on both the external and internal leaflet of the vesicle, *SI Appendix*, Fig. S13. (Also imaged by negatively stained TEM, *SI Appendix*, Fig. S15). After 2 h of incubation internalization of Aβ oligomers is widespread. After 36 h of incubation, there are numerous fibrils formed outside the vesicles, *SI Appendix*, Figs. S13 and S14. Surprisingly, although

the cryo-EM and cryo-ET indicate oligomers concentrated within the vesicles, there is little evidence of fibrils forming, despite the high concentrations of oligomers. The low levels/absence of fibril formation suggests that appreciable amounts of Aβ monomer do not enter the vesicle which are required for the growth of oligomers into fibrils.

To conclude, using cryo-ET we have obtained 3D images, at nanoscale resolution, revealing the interaction of Aβ42 with the membranes of cell-derived vesicles. Our results reveal markedly different modes of interaction dependent on the assembly state of Aβ42. Aβ oligomers including annular and CLEOs exhibit extensive association with the sEV membrane, carpeting the surface, insertion within the membrane and internalization, which suggests active penetration and uptake of Aβ oligomers. In contrast, Aβ monomers and preformed fibrils have minimal impact on the membrane. These findings align with studies showing cytotoxicity only for oligomeric Aβ (4–8) which disrupt membrane integrity and cause the influx of Ca^{2+} and other ions (12, 17–19). Our studies also show that sEVs, including exosomes, can serve as carriers of a concentrated reservoir of toxic Aβ oligomers. Although an in vitro study, our 3D nanoscale images of Aβ oligomers interacting with extracellular vesicles is an important advance, in the future we hope to obtain cellular imaging of Aβ oligomers at the synapse

Materials and Methods

See *SI Appendix* for details. Briefly, sEVs were separated from the cell medium by differential ultracentrifugation, a method optimized to maximize yield while minimizing contamination from cellular debris and damaged vesicles (58). The resulting sEVs preparations were resuspended in phosphate-buffered saline (PBS) at pH 7.4, for subsequent experimental analysis. Lyophilized Aβ42 was solubilized at pH 10 and eluted through a size exclusion column to generate monomeric Aβ42. Assembly of Aβ42 into oligomers, which includes a mixture of small oligomers, CLEOs, and annular oligomers, were collected toward the end of the prefibrillar lag-phase, *SI Appendix*, Fig. S16. While fibrils were collected at the plateau/equilibrium stage of assembly. We note Aβ nano-molar levels in vivo would be difficult to image effectively by cryo-ET, instead Aβ42 was incubated with vesicles at 10 μM monomer equivalent. Using a method designed for high-resolution imaging and excellent structural preservation, a volume (4 μL) of the sEV suspension was applied to cryo-EM grids and vitrified in liquid ethane. A Titan Krios microscope running at 300 kV was used to acquire a 2D tilt series, and tomograms were computationally rebuilt to provide 3D volumes. Creating highly contrasting 3D images of extracellular vesicles with Aβ assemblies in near native conditions.

Data, Materials, and Software Availability. A representative tomogram of extracellular vesicles with Aβ42 oligomers EMB-58700 (61) has been deposited in the Electron Microscopy Data Bank. All other data are present in the paper and supporting information.

ACKNOWLEDGMENTS. Biotechnology and Biological Sciences Research Council project grant BB/Y001931/1. National Natural Science Foundation of China, Grant No. 32501123. Nora B. Cronin for assistance with cryo-EM image acquisition, LonCEM Facility, The Francis Crick Institute, London, UK. Electron Bio-Imaging Centre (eBIC), Diamond Light Source, Oxford, UK.

Author affiliations: [a]Centre for Molecular and Cellular Biology, Department of Biochemistry, School of Biological and Behavioural Sciences, Queen Mary University of London, London E1 4NS, United Kingdom; [b]Wuhan Institute for Neuroscience and Neuroengineering, College of Life Sciences, South-Central Minzu University, Wuhan 430074, China; and [c]Center for Microscopy and Image Analysis, University of Zurich, Zurich CH-8006, Switzerland

1. M. Prince *et al.*, World Alzheimer report 2015: The Global Impact of Dementia–An analysis of prevalence, incidence, cost and trends. *Alzheimer's Disease International* (2015), vol. 84, 10.1111/j.0963-7214.2004.00293.x.
2. D. J. Selkoe, J. Hardy, The amyloid hypothesis of Alzheimer's disease at 25 years. *EMBO Mol. Med.* **8**, 595–608 (2016).
3. J. A. Hardy, G. A. Higgins, Alzheimer's disease: The amyloid cascade hypothesis. *Science* **256**, 184–185 (1992).
4. I. Benilova, E. Karran, B. De Strooper, The toxic Aβ oligomer and Alzheimer's disease: An emperor in need of clothes. *Nat. Neurosci.* **15**, 349–357 (2012).
5. E. N. Cline, M. A. Bicca, K. L. Viola, W. L. Klein, The amyloid-beta oligomer hypothesis: Beginning of the third decade. *J. Alzheimers Dis.* **64**, S567–S610 (2018).
6. M. P. Lambert *et al.*, Diffusible, nonfibrillar ligands derived from A beta(1–42) are potent central nervous system neurotoxins. *Proc. Natl. Acad. Sci. U.S.A.* **95**, 6448–6453 (1998).
7. D. M. Walsh *et al.*, Naturally secreted oligomers of amyloid beta protein potently inhibit hippocampal long-term potentiation in vivo. *Nature* **416**, 535–539 (2002).
8. T. Yasumoto *et al.*, High molecular weight amyloid beta(1–42) oligomers induce neurotoxicity via plasma membrane damage. *Faseb. J.* **33**, 9220–9234 (2019).
9. J. H. Viles, Imaging amyloid-beta membrane interactions: Ion-channel pores and lipid-bilayer permeability in Alzheimer's disease. *Angew. Chem. Int. Edit.* **62**, e202215785 (2023), 10.1002/anie.202215785.
10. S. M. Butterfield, H. A. Lashuel, Amyloidogenic protein-membrane interactions: Mechanistic insight from model systems. *Angew. Chem. Int. Ed. Engl.* **49**, 5628–5654 (2010).
11. Y. Tian, R. Liang, A. Kumar, P. Szwedziak, J. H. Viles, 3D-visualization of amyloid-β oligomer interactions with lipid membranes by cryo-electron tomography. *Chem. Sci.* **12**, 6896–6907 (2021).
12. R. N. Liang *et al.*, Amyloid-β oligomers, curvilinear and annular assemblies, imaged by cryo-ET, cryo-EM, and AFM. *Sci. Adv.* **11**, eadx9030 (2025).
13. I. Bezprozvanny, M. P. Mattson, Neuronal calcium mishandling and the pathogenesis of Alzheimer's disease. *Trends Neurosci.* **31**, 454–463 (2008).
14. J. L. Farber, The role of calcium ions in toxic cell injury. *Environ. Health Perspect.* **84**, 107–111 (1990).
15. M. P. Mattson *et al.*, Beta-amyloid peptides destabilize calcium homeostasis and render human cortical-neurons vulnerable to excitotoxicity. *J. Neurosci.* **12**, 376–389 (1992).
16. S. Magi *et al.*, Intracellular calcium dysregulation: Implications for Alzheimer's disease. *Biomed. Res. Int.* **2016**, 6701324 (2016).
17. A. Demuro *et al.*, Calcium dysregulation and membrane disruption as a ubiquitous neurotoxic mechanism of soluble amyloid oligomers. *J. Biol. Chem.* **280**, 17294–17300 (2005).
18. Y. Tian, Q. Shang, R. Liang, J. H. Viles, Copper (II) can kinetically trap arctic and Italian amyloid-β40 as toxic oligomers, mimicking Cu (II) binding to wild-type amyloid-β42: Implications for familial Alzheimer's disease. *JACS Au* **4**, 578–591 (2024).
19. Y. Tian *et al.*, The p3 peptides (Aβ) rapidly form amyloid fibrils that cross-seed with full-length Aβ. *Nat. Commun.* **16**, 2040 (2025).
20. P. Flagmeier *et al.*, Direct measurement of lipid membrane disruption connects kinetics and toxicity of Aβ42 aggregation. *Nat. Struct. Mol. Biol.* **27**, 886–891 (2020).
21. P. Flagmeier *et al.*, Ultrasensitive measurement of Ca2+ influx into lipid vesicles induced by protein aggregates. *Angew. Chem. Int. Ed.* **56**, 7750–7754 (2017).
22. D. C. Bode, M. Freeley, J. Nield, M. Palma, J. H. Viles, Amyloid-β oligomers have a profound detergent-like effect on lipid membrane bilayers, imaged by atomic force and electron microscopy. *J. Biol. Chem.* **294**, 7566–7572 (2019).
23. D. Matthes, B. L. de Groot, Molecular dynamics simulations reveal the importance of amyloid-beta oligomer β-sheet edge conformations in membrane permeabilization. *J. Biolog. Chem.* **299**, 103034 (2023).
24. S. Ciudad *et al.*, Abeta(1–42) tetramer and octamer structures reveal edge conductivity pores as a mechanism for membrane damage. *Nat. Commun.* **11**, 3014 (2020).
25. N. Arispe, E. Rojas, H. B. Pollard, Alzheimer disease amyloid beta protein forms calcium channels in bilayer membranes: Blockade by tromethamine and aluminum. *Proc. Nat. Acad. Sci.* **90**, 567–571 (1993).
26. D. C. Bode, M. D. Baker, J. H. Viles, Ion channel formation by amyloid-β42 oligomers but not amyloid-β40 in cellular membranes. *J. Biol. Chem.* **292**, 1404–1413 (2017).
27. H. Lin, R. Bhatia, R. Lal, Amyloid β protein forms ion channels: Implications for Alzheimer's disease pathophysiology. *FASEB J.* **15**, 2433–2444 (2001).
28. B. Mroczko, M. Groblewska, A. Litman-Zawadzka, J. Kornhuber, P. Lewczuk, Cellular receptors of amyloid beta oligomers (AbetaOs) in Alzheimer's disease. *Int. J. Mol. Sci.* **19**, 1884 (2018).
29. M. Gonzalez-Garcia, G. Fusco, A. De Simone, Membrane interactions and toxicity by misfolded protein oligomers. *Front. Cell Dev. Biol.* **9**, 642623 (2021).
30. S. A. Purro, A. J. Nicoll, J. Collinge, Prion protein as a toxic acceptor of amyloid-β oligomers. *Biol. Psychiatry* **83**, 358–368 (2018).
31. T. Kim *et al.*, Human LilrB2 Is a β-amyloid receptor and its murine homolog PirB regulates synaptic plasticity in an Alzheimer's model. *Science* **341**, 1399–1404 (2013).
32. G. K. Gouras *et al.*, Intraneuronal Aβ42 accumulation in human brain. *Am. J. Pathol.* **156**, 15–20 (2000).
33. T. A. Bayer, O. Wirths, Intracellular accumulation of amyloid-Beta-a predictor for synaptic dysfunction and neuron loss in Alzheimer's disease. *Front. Aging Neurosci.* **2**, 1359 (2010).
34. F. M. LaFerla, K. N. Green, S. Oddo, Intracellular amyloid-β in Alzheimer's disease. *Nat. Rev. Neurosci.* **8**, 499 (2007).
35. S. Jin *et al.*, Amyloid-β (1–42) aggregation initiates its cellular uptake and cytotoxicity. *J. Biol. Chem.* **291**, 19590–19606 (2016).
36. A. Y. Lai, J. McLaurin, Mechanisms of amyloid-beta peptide uptake by neurons: The role of lipid rafts and lipid raft-associated proteins. *Int. J. Alzheimer's Disease* **2011**, 548380 (2011).
37. X. Bi, C. M. Gall, J. Zhou, G. Lynch, Uptake and pathogenic effects of amyloid beta peptide 1–42 are enhanced by integrin antagonists and blocked by NMDA receptor antagonists. *Neuroscience* **112**, 827–840 (2002).
38. R. G. Nagele, M. R. D'Andrea, W. J. Anderson, H. Y. Wang, Intracellular accumulation of β-amyloid in neurons is facilitated by the α7 nicotinic acetylcholine receptor in Alzheimer's disease. *Neuroscience* **110**, 199–211 (2002).
39. C. J. Yu, E. Nwabuisi-Heath, K. Laxton, M. J. LaDu, Endocytic pathways mediating oligomeric Aβ42 neurotoxicity. *Mol. Neurodegener.* **5**, 19 (2010).

40. E. Wesén, G. D. M. Jeffries, M. Matson Dzebo, E. K. Esbjörner, Endocytic uptake of monomeric amyloid-β peptides is clathrin- and dynamin-independent and results in selective accumulation of Aβ(1–42) compared to Aβ(1–40). *Sci. Rep.* **7**, 2021 (2017).
41. S. Jaye, U. S. Sandau, J. A. Saugstad, Clathrin mediated endocytosis in Alzheimer's disease: Cell type specific involvement in amyloid beta pathology. *Front. Aging Neurosci.* **16**, 1378576 (2024).
42. K. K. Kandimalla, O. G. Scott, S. Fulzele, M. W. Davidson, J. F. Poduslo, Mechanism of neuronal versus endothelial cell uptake of Alzheimer's disease amyloid beta protein. *PLoS One* **4**, e4627 (2009).
43. S. Andrade, J. A. Loureiro, M. C. Pereira, The role of amyloid β-biomembrane interactions in the pathogenesis of Alzheimer's disease: Insights from liposomes as membrane models. *Chemphyschem* **22**, 1547–1565 (2021).
44. M. A. G. Gilbert *et al.*, CryoET of β-amyloid and tau within postmortem Alzheimer's disease brain. *Nature* **631**, 913 (2024).
45. G. van Niel, G. D'Angelo, G. Raposo, Shedding light on the cell biology of extracellular vesicles. *Nat. Rev. Mol. Cell Biol.* **19**, 213–228 (2018).
46. T. Skotland, N. P. Hessvik, K. Sandvig, A. Llorente, Exosomal lipid composition and the role of ether lipids and phosphoinositides in exosome biology. *J. Lipid Res.* **60**, 9–18 (2019).
47. J. C. Akers, D. Gonda, R. Kim, B. S. Carter, C. C. Chen, Biogenesis of extracellular vesicles (EV): Exosomes, microvesicles, retrovirus-like vesicles, and apoptotic bodies. *J. Neurooncol.* **113**, 1–11 (2013).
48. F. Xu *et al.*, Composition, functions, and applications of exosomal membrane proteins. *Front. Immunol.* **15**, 1408415 (2024).
49. L. Rajendran *et al.*, Alzheimer's disease β-amyloid peptides are released in association with exosomes. *Proc. Natl. Acad. Sci. U.S.A.* **103**, 11172–11177 (2006).
50. K. Yuyama, Y. Igarashi, Exosomes as carriers of Alzheimer's amyloid-ß. *Front. Neurosci.* **11**, 229 (2017).
51. T. Malm, S. Loppi, K. M. Kanninen, Exosomes in Alzheimer's disease. *Neurochem. Int.* **97**, 193–199 (2016).
52. P. Joshi, L. Benussi, R. Furlan, R. Ghidoni, C. Verderio, Extracellular vesicles in Alzheimer's disease: Friends or foes? Focus on aβ-vesicle interaction. *Int. J. Mol. Sci.* **16**, 4800–4813 (2015).
53. K. Yuyama *et al.*, A potential function for neuronal exosomes: Sequestering intracerebral amyloid-β peptide. *FEBS Letters* **589**, 84–88 (2015).
54. R. H. Takahashi *et al.*, Intraneuronal Alzheimer Aβ42 accumulates in multivesicular bodies and is associated with synaptic pathology. *Am. J. Pathol.* **161**, 1869–1879 (2002).
55. M. Sardar Sinha *et al.*, Alzheimer's disease pathology propagation by exosomes containing toxic amyloid-beta oligomers. *Acta Neuropathol.* **136**, 41–56 (2018).
56. A. G. Thompson *et al.*, Extracellular vesicles in neurodegenerative disease–pathogenesis to biomarkers. *Nat. Rev. Neurol.* **12**, 346–357 (2016).
57. A. Khursheed, J. H. Viles, Impact of membrane phospholipids and exosomes on the kinetics of amyloid-β Fibril assembly. *J. Mol. Biol.* **436**, 168464 (2024).
58. C. Thery, S. Amigorena, G. Raposo, A. Clayton, Isolation and characterization of exosomes from cell culture supernatants and biological fluids. *Curr. Protoc. Cell Biol.* **Chapter 3**, Unit 3 22 (2006).
59. K. Yuyama, H. Sun, S. Mitsutake, Y. Igarashi, Sphingolipid-modulated exosome secretion promotes clearance of amyloid-β by microglia. *J. Biol. Chem.* **287**, 10977–10989 (2012).
60. Y. Sugiura, K. Ikeda, M. Nakano, High membrane curvature enhances binding, conformational changes, and fibrillation of amyloid-β on lipid bilayer surfaces. *Langmuir* **31**, 11549–11557 (2015).
61. A. Khursheed *et al.*, Representative tomogram of extracellular vesicles with Aβ42 oligomers. EMDB. https://www.ebi.ac.uk/emdb/EMD-EMB-58700. Deposited 26 June 2026.